An Active Balancer of Currents for Bipolar DC Power Grids

Vitor Monteiro
Centro ALGORITMI / LASI
University of Minho
Guimaraes, Portugal
vmonteiro@dei.uminho.pt

Sergio Coelho
Centro ALGORITMI / LASI
University of Minho
Guimaraes, Portugal
sergio.coelho@algoritmi.uminho.pt

Saghir Amin
Centro ALGORITMI / LASI
University of Minho
Guimaraes, Portugal
id11315@alunos.uminho.pt

Muhammad Awais
Centro ALGORITMI / LASI
University of Minho
Guimaraes, Portugal
id11380@alunos.uminho.pt

Pedro Brito
Centro ALGORITMI / LASI
University of Minho
Guimaraes, Portugal
pg54149@alunos.uminho.pt

Joao L. Afonso
Centro ALGORITMI / LASI
University of Minho
Guimaraes, Portugal
jla@dei.uminho.pt

***Abstract*—DC power grids (DCPGs) are gaining more significance, predominantly due to the natural DC operation of technologies such as renewables, energy storage systems, and electric vehicles. Particularly, thanks to power electronics, bipolar DCPGs are gaining more preponderance since they enable reducing power losses, increasing power density, and averting power quality problems of AC power grids. Also, by adding power electronics, it is possible to establish different voltage levels to be adapted to different DC loads. However, since it is difficult to ensure balanced operating power for all loads in a bipolar DCPG, current imbalances emerge. This paper proposes an active balancer of currents (ABC), which is used to ensure balanced source currents in bipolar DCPGs, along with the corresponding power control theory. The ABC has two two-wire power interfaces, both linked in shunt to the DCPG, and both can be controlled to operate in bidirectional buck or boost modes. The validation was performed considering distinct current imbalances from the load point of view, permitting the verification of the correct operation of the ABC for balancing the current in the power source.**

Keywords—Active Balancer of Currents, Bipolar DC Power Grids, DC-DC Power Electronics Converters

I. Introduction

The modernization of power grids is an unquestionable point that is under the concern of the whole world [1], [2]. This is due to several factors, which undoubtedly include the new breakthroughs on semiconductor technologies, massification associated with the introduction of renewable energy sources (RES), and the change in mobility paradigm, increasingly focused on the different types of electric vehicles (EV) [3], [4]. This is also valid to the change to a decentralized paradigm of energy production, progressing towards a more inclusive and interactive power grid, where the consumers also play a role in the quality and stability of the grid and smart power meters are indispensable [5]. Investing in renewables and electric mobility, both at private and public levels at different power levels, is certainly necessary to meet energy environmental targets [6]. However, this bet involves a set of challenges for transmission and distribution system operators, where the possibility of integrating energy storage systems (ESS) to balance demand and supply is fundamental, mainly considering the dependence on climatic conditions that affect production from renewables [7], [8]. Added to this analysis is the introduction of more and more electronic devices with specific requirements in terms of power and voltage levels.

Associated with the decentralization of power production, microgrids emerge, which can operate in collaborative mode with the main power grid or in islanded mode [9], [10]. On the other hand, from the point of view of the technological development of power electronics systems, most of the above-mentioned technologies operate natively in DC. Therefore, DC power grids (DCPG) are also a possibility, offering the option of reducing the number of converters and, as a consequence, increasing the efficiency of the system as a whole [11], [12], [13]. A detailed review about classification, issues and implementation challenges, control strategies, and future trends regarding microgrids is presented in [14].

Traditional DCPGs are based on a two-wire system, allowing only one voltage to be established (i.e., unipolar DCPG). However, to facilitate the integration of different technologies with different voltage requirements, bipolar DCPG are also possible to implement, including the opportunity of a bidirectional interface between them [15]. In fact, in addition to offering the chance of two different voltage levels (normally one is double the other), redundancy is also an importance feature, as well as in case of failure of one voltage level (e.g., failure in one of the wires), the other is not compromised [16]. This advantage can be very important when designing the DC-DC converters to interface with the bipolar DCPG [17]. In addition, power electronics converter topologies can also be used for operating in faulty conditions [18].

Analyzing the technologies that interface with the bipolar DCPG, the possibility of symmetrical voltage levels is very relevant. Fig. 1 presents a bipolar DCPG derived from an AC power grid, i.e., through a three-phase AC-DC power converter followed by a three-level DC-DC stage along with some exemplificative technologies interfacing the DCPG.

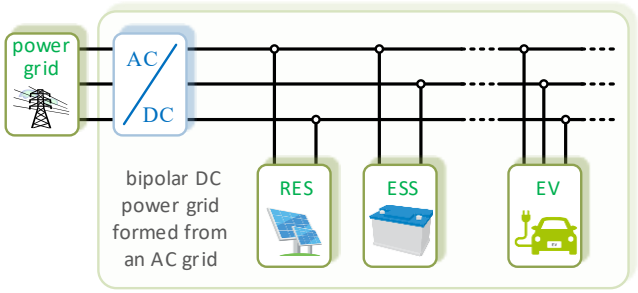


Fig. 1. Bipolar DC power grid, formed from an AC power grid, and interfaced by some exemplificative technologies aiming to highlight the versatility regarding voltage levels.

These power stages can be isolated or not, however, high-frequency isolation is preferable and mandatory according to specific standards. To highlight the versatility of the DCPG regarding voltage levels, it is represented: (i) the RES interfacing two-wires (positive and negative); (ii) the ESS interfacing two-wires (positive and neutral); (iii) the EV interfacing three-wires (positive, neutral, and negative). From the bipolar DCPG point of view, this configuration can be harmful, as it is not possible to always guarantee that the RMS current on both positive and negative lines is equal [19]. This problem introduces imbalances that compromise the correct operation of the AC-DC power converter, which is linked to the DC-DC used to create the bipolar DCPG, introducing a power quality problem. This can be mitigated by using an active balancer of currents (ABC) in parallel with the DCPG, as proposed in this paper. Although a bipolar DCPG is physically composed of three wires, the proposed parallel DC-DC ABC solution is based on two separates two-wire interfaces. Supported by this introductory contextualization, the essential contributions of the paper can be distinguished as: (i) novel power electronics topology of DC-DC ABC, composed of two power converters sharing a common DC-link, which is used for balancing the source currents in bipolar DCPG; (ii) power control theory for balancing power in bipolar DCPG, by controlling the currents. The goal is to ensure balanced currents in the positive and negative wires and zero current in the neutral wire from the source point of view, while the currents in the load can be imbalanced; (iii) the parallel DC-DC ABC has two two-wire power interfaces, and both can operate in buck or boost mode, depending on the top or bottom unbalancing on the load side; (iv) current control strategy for both interfaces, when in buck or boost mode, ensuring current balancing and DC-link voltage control (established individually by one of the interfaces), depending on the top or bottom unbalancing on the load side.

The operating principle of the proposed DC-DC ABC is introduced in section II, highlighting the different operating modes, while the details about the control algorithms and digital implementation are introduced in section III. Computational validation is depicted in section IV for the most relevant cases, and conclusions are presented in section V.

II. Operating Principle of the Proposed DC-DC Active Balancer of Currents

The electrical schematic that illustrates the proposed DC-DC ABC for application in bipolar DCPG is shown in Fig. 2. As can be seen, one of the interfaces (power converter DC-DC #1) connects directly between the positive and negative wires, while the other interface (power converter DC-DC #2) connects directly between the neutral and negative wires. A common DC-link is shared by the two DC-DC power converters and both interfaces allow bidirectional operation, either in buck or boost modes depending on unbalances on the loads (i.e., it is not the case that both interfaces operate simultaneously in buck or boost mode). The operation in buck or boost mode depends on the power unbalances in the loads. Due to the proposed configuration of the power electronics converters, it is not necessary to guarantee galvanic isolation between the power interfaces DC-DC #1 and DC-DC #2.

As the AC-DC power converter and its controller are responsible for generating the bipolar DCPG, they must ensure that the DC voltages and power remain balanced. For

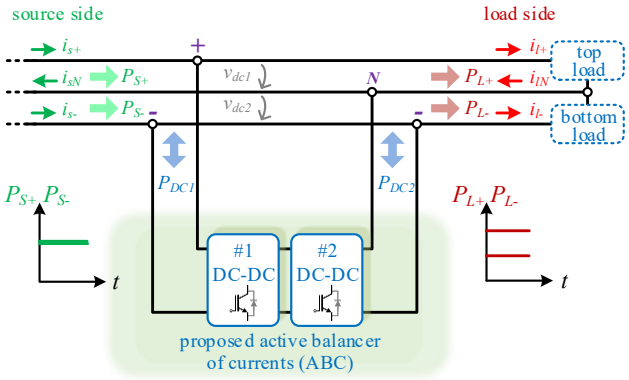


Fig. 2. Electrical schematic that illustrates the proposed active balancer of currents (ABC) for applications in bipolar DC power grids (DCPGs).

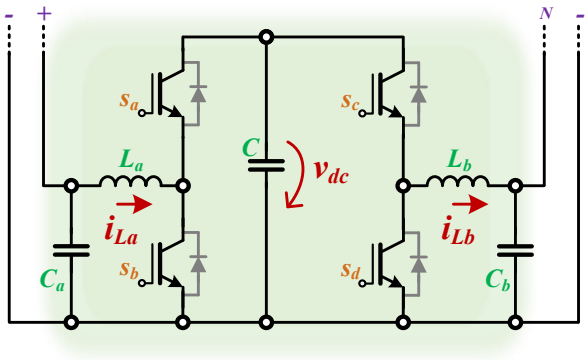


Fig. 3. Topologies of DC-DC #1 and DC-DC #2 power converters for the proposed active balancer of currents (ABC) for application in bipolar DC power grids (DCPGs).

power balancing, it is necessary to control the current so that it is equal on the positive and negative wires, while remaining zero on the neutral wire. The DC-DC #1 can receive (boost mode) or supply current (buck mode) in connection with the positive wire, while DC-DC #2 can receive (boost mode) or supply current (buck mode) in connection with the neutral wire. For both DC-DC, proving power to the DCPG means the operation in buck mode, while receiving power means the operation in boost mode. In this way, in the bipolar DCPG side, it is possible to guarantee zero current on the neutral wire and the same value of current on the positive and negative wires. The control of the DC-link shared by both DC-DC power converters is carried out by the DC-DC stage that operates in boost mode, i.e., it can be either interface #1 or interface #2. As the DC-DC #1 is linked with positive and negative wires, the voltage on the shared DC-link must be greater than the sum of the nominal voltages v_{dc1} and v_{dc2}. Only in this way, it can be guaranteed the correct operation of both DC-DC power converters. Regarding the interface with the DCPG, as the input voltage on the DC-DC #1 is twice the voltage on the DC-DC #2, the reference current for each of the interfaces must take this aspect into account to maintain the same power value on both interfaces. Basically, there are two modes of operation depending on the imbalance: (i) the operating power on the top load is higher than the operating power on the bottom load; (ii) the operating power on the top load is lower than the operating power on the bottom load.

The power electronics topologies of DC-DC #1 and DC-DC #2 power converters for the proposed DC-DC ABC for application in bipolar DCPGs are presented in Fig. 3. As shown, four IGBTs are used in total, and *LC* coupling filters are used in both power interfaces. The representation of the

current reflects the operation of DC-DC #1 in boost mode and DC-DC #2 in buck mode. In fact, for the validation purpose, the current sensors placement is maintained unchanged.

To exemplify the operating principle of the proposed DC-DC ABC, Fig. 4 presents a representation of the currents, assuming imbalanced currents in the load side. Therefore, it is assumed a current with a value of y A in the positive wire, z A in the negative wire, and as expected, the difference $z - y$ A is reflected on the neutral. For ensuring balanced currents in the source side, i.e., $\pm x$ A in the positive and negative wires and 0 A in the neutral wire, the DC-DC ABC must operate with the DC-DC #1 in boost mode controlling a current with a value of $x - y$ A, while the DC-DC #2 must operate in buck mode controlling a current with a value of $x - z$ A. In the negative common wire of the DC-DC ABC, the current is divided and has a value of $-((x - y)/2)$ A.

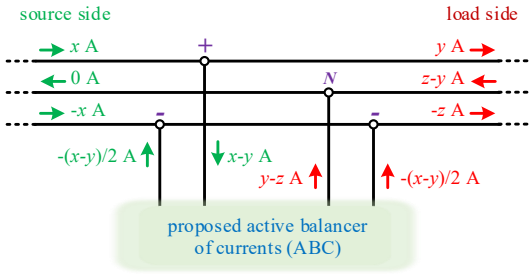


Fig. 4. Representation of the currents, assuming imbalanced currents in the load side and, due to the proposed active balancer of currents (ABC), with balanced currents in the source side.

III. Digital Control of the Proposed DC-DC Active Balancer of Currents

During the imbalanced current operation of the load, when the load current in the negative wire (i_{L-}) is higher than the current in the positive wire (i_{L+}), the IGBTs s_a and s_d are always turned *off*, while IGBTs s_b and s_c are switching. This situation corresponds to the operation of the DC-DC #1 in boost mode and to the operation of the DC-DC #2 in buck mode. The references of current for DC-DC #1 and DC-DC #2 are defined, respectively, by:

$$i_{dc\#1}{}^{*} = \frac{P_{L+}}{\overline{v_{dc1}} + \overline{v_{dc2}}} + i_{dc-link}\,, \tag{1}$$

$$i_{dc\#2}{}^{*} = \frac{P_{L+}}{\overline{v_{dc2}}}, \tag{2}$$

where $i_{dc\text{-}link}$ is obtained from a PI controller used to regulate the DC-link voltage. As previously mentioned, the DC link voltage must be regulated independently of the operation mode. This task is performed by the DC-DC power interface operating in boost mode. Accordingly, this power converter is responsible for controlling both the input current and the DC-link voltage. For simplicity, a PI controller is used to regulate the DC-link voltage. Based on such references of current and the analysis of the power electronics topology, predictive-based current controls are established for both power interfaces, which are defined by:

$$i_{dc\#1}[n] = i_{dc\#1}{}^{*}[n] + (b^{*}[n] - v_{dc1}[n] - v_{dc2}[n])\frac{T_s}{L_{\#1}}, \tag{3}$$

$$i_{dc\#2}[n] = i_{dc\#2}{}^{*}[n] - (c^{*}[n] - v_{dc2}[n])\frac{T_s}{L_{\#2}}, \tag{4}$$

where $b[n]$ and $c[n]$ correspond to the modulators used in the pulse-width modulation (PWM) to be compared with the respective carriers.

A similar reasoning is applied during the imbalanced operation of the load when the load current in the negative wire (i_{L-}) is lower than the current in the positive wire (i_{L+}). In this case, IGBTs s_b and s_c are always turned off and IGBTs s_a and s_d. are switching. Consequently, DC-DC #1 operates in buck mode, while DC-DC #2 operates in boost mode. In this scenario, the references of current for DC-DC #1 and DC-DC #2 are defined, respectively, by:

$$i_{dc\#1}{}^{*} = -\frac{P_{L-}}{\overline{v_{dc1}} + \overline{v_{dc2}}}, \tag{5}$$

$$i_{dc\#2}{}^{*} = -\frac{P_{L-}}{\overline{v_{dc1}} + \overline{v_{dc2}}} - i_{dc-link}\,, \tag{6}$$

where the negative signal is just related to the original position of the current sensors on both sides (cf. Fig. 2 and Fig. 3). In this case, the predictive-based current controls are defined by:

$$i_{dc\#1}[n] = i_{dc\#1}{}^{*}[n] + (a^{*}[n] - v_{dc1}[n] - v_{dc2}[n])\frac{T_s}{L_{\#1}}, \tag{7}$$

$$i_{dc\#2}[n] = i_{dc\#2}{}^{*}[n] - (d^{*}[n] - v_{dc2}[n])\frac{T_s}{L_{\#2}}, \tag{8}$$

where $a[n]$ and $d[n]$ correspond to the modulators compared with the respective carriers. A flowchart is presented in Fig. 5 which aims to facilitate understanding of how the proposed control algorithm is implemented.

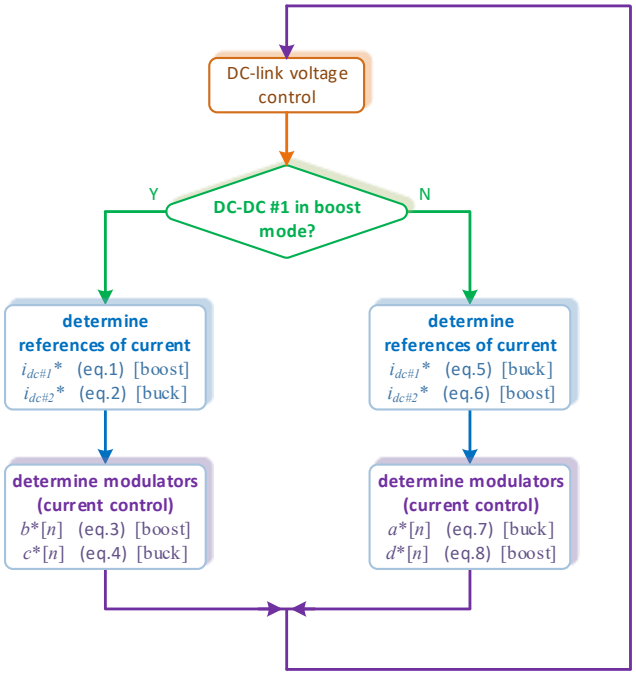


Fig. 5. Flowchart of the control algorithm for the proposed active balancer of currents (ABC).

IV. Computational Validation of the Proposed DC-DC Active Balancer of Currents

For validating the proposed DC-DC ABC, a complete simulation model was developed in PSIM software. The main electrical characteristics used to perform the simulation are listed in Table I. These values were considered just for the

purpose of validating the proposed DC-DC ABC, therefore, they can be adapted for other scenarios.

Table I. Electrical characteristics used in the PSIM simulation for validating the proposed DC-DC active balancer of currents (ABC).

PARAMETER	LABEL	VALUE	UNIT
Switching Frequency	f_{sw}	80	kHz
DC Power Grid Voltage	v_{dc1}, v_{dc2}	400+400	V
DC-link Voltage	v_{dc}	900	V
L filter	L_a, L_b	5	mH
C filter	C_a, C_b	5	mF
P nominal	P_N	24	kW

A. *Power P_{L+} Lower than Power P_{L-}*

In this mode of operation, DC-DC #2 operates with current control in buck mode, forcing an input current into the negative wire. On the other hand, DC-DC #1 operates in boost mode with double inner and outer control, i.e., a current control loop forcing an output current from the positive wire and a voltage control loop on the shared DC-link. This voltage control is mandatory for ensuring the correct operation of DC-DC #2 in buck mode. Fig. 6 shows a result in this situation, where it is possible to verify the currents on the source (i_{s+}, i_{sN}, i_{s-}) and load side (i_{l+}, i_{lN}, i_{l-}). As shown, the current i_{l+} is lower than the current i_{l-}, meaning a negative current (i_{lN}) on the neutral wire in the load side. The negative representation of the current is just related to the position of the current sensor. With the proposed DC-DC ABC, the currents on the source side are balanced, meaning that the value of the currents i_{s+} and i_{s-} are equal and the current i_{sN} is zero. This analysis is also valid according to the position of the current sensors.

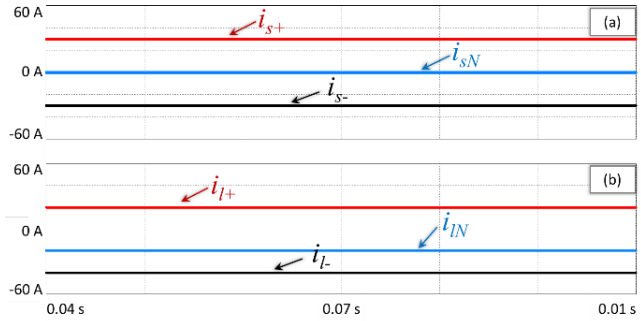


Fig. 6. Validation considering that the power in the top load is lower than the power in the bottom load: (a) Currents on the DCPG side (i_{s+}, i_{sN}, i_{s-}); (b) Currents on the load side (i_{l+}, i_{lN}, i_{l-}).

Fig. 7 shows a detail of the currents on the source side (i_{s+}, i_{sN}, i_{s-}), highlighting the average values and the ripple. As observed, the currents are balanced for the same average value on the positive (i_{s+}) and negative (i_{s-}) wires, while it is zero in the neutral wire (i_{sN}). In this operation mode, in terms of average and ripple values, i_{s-} corresponds to i_{sN} minus i_{s+}. As shown, four different stages are identified (i to iv). The currents in the coupling filters L_a and L_b are presented in Fig. 8, while the detail of the ripple of such currents is depicted in Fig. 9, in accordance with the switching of the IGBTs *b* and *c* (s_b and s_c). In this particular operation case, on the load side, as i_{l+} is half of i_{l-}, the current in L_a is half of the current in L_b, since DC-DC #1 is linked to 800 V and DC-DC #2 to 400 V, operating, respectively in boost and buck mode. The imbalance will only influence the power to be balanced, but the current in L_a (i_{La}) is half of the current in L_b (i_{Lb}) due to the fact that one input voltage is twice the value of the other output voltage. As shown, in both cases, when the IGBTs are *on*, the inductors store energy, while when the IGBTs are *off*, the energy is delivered to the circuit.

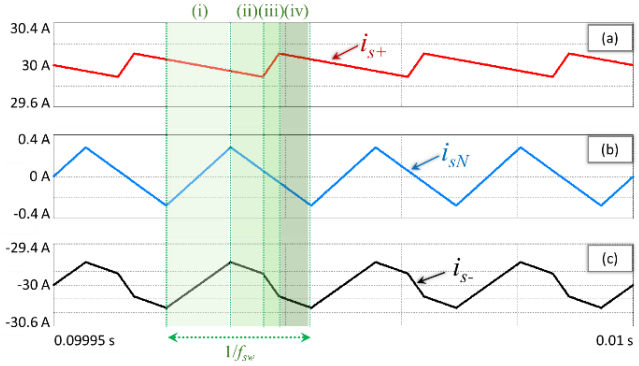


Fig. 7. Validation considering that the power in the top load is lower than the power in the bottom load, showing the detail of the average and ripple values: (a) Current i_{s+}; (b) Current i_{sN}; (c) Current i_{s-}.

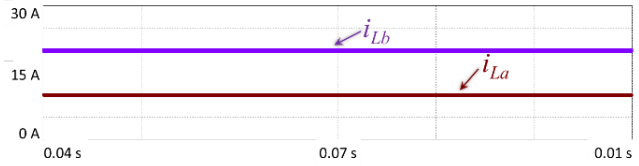


Fig. 8. Validation considering that the power in the top load is lower than the power in the bottom load, showing the currents in the coupling inductors, namely i_{La} and i_{Lb}.

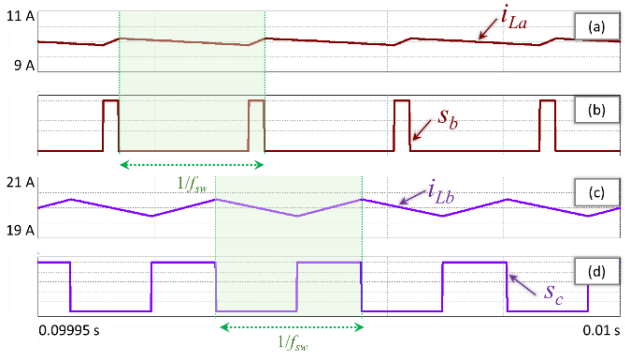


Fig. 9. Validation considering that the power in the top load is lower than the power in the bottom load, showing the detail of the ripple in the currents i_{La} and i_{Lb}, as well as the PWM of the IGBTs s_b and s_c.

Fig. 10 shows the voltage of the DCPG, namely v_{dc1} and v_{dc2}, as well as the DC-link voltage (v_{dc}) shared between DC-DC #1 and DC-DC #2. As shown, the nominal voltage of v_{dc1} and v_{dc2} is 400 V, while v_{dc} is controlled for an average value of 900 V, which is a superior value than v_{dc1} or v_{dc2}. This is mandatory for ensuring the operation of DC-DC #1 in boost mode. Fig. 11 shows the results obtained in transient-state to demonstrate the operation of the DC-DC ABC before and after the compensation. Initially, the DC-DC ABC is not operating, and the source currents are the same as the load currents and at $t = 0.06$ s, the DC-DC ABC is turned-on, resulting in the current compensation, meaning that the source currents are balanced, while the load currents continue the same.

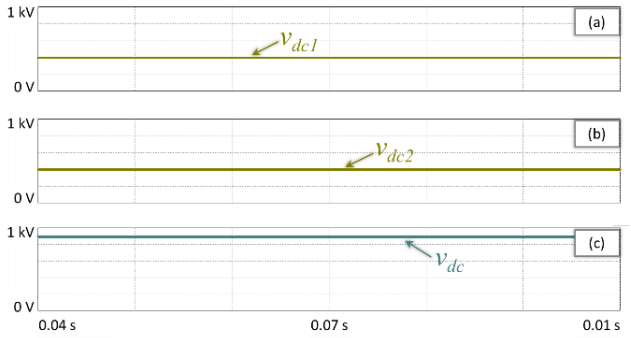


Fig. 10. Validation considering that the power in the top load is lower than the power in the bottom load, showing the transient-state to demonstrate the operation before and after the compensation: (a) DC-link voltage v_{dc1}; (b) DC-link voltage v_{dc2}; (c) DC-link voltage v_{dc}.

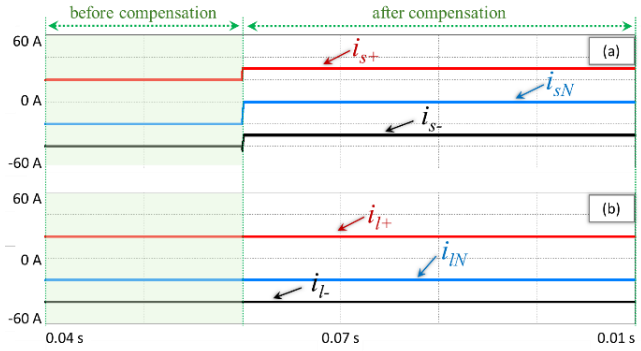


Fig. 11. Validation considering that the power in the top load is lower than the power in the bottom load, showing the voltages: (a) Currents on the DCPG side (i_{s+}, i_{sN}, i_{s-}); (b) Currents on the load side (i_{l+}, i_{lN}, i_{l-}).

B. *Power P_{L+} Lower than Power P_{L-}*

In this mode of operation, DC-DC #1 operates with current control in buck mode, forcing an input current into the positive wire. On the other hand, DC-DC #2 operates in boost mode with double inner and outer control, i.e., a current control loop forcing an output current from the neutral wire and a voltage control loop on the shared DC-link. The DC-link voltage control is indispensable to guarantee the correct operation of DC-DC #1 in buck mode. Fig. 12 shows a result in this situation, where it is possible to verify the currents on the source (i_{s+}, i_{sN}, i_{s-}) and load side (i_{l+}, i_{lN}, i_{l-}). As shown, the current i_{l+} is higher than the current i_{l-}, meaning a positive current on the neutral wire in the load side (i_{lN}). Due to the operation of the DC-DC ABC, the currents on the source side are balanced, meaning that the value of the currents i_{s+} and i_{s-} are equal and the current i_{sN} is zero. It is important to note that this analysis is performed, and it is valid according to the defined position of the current sensors (cf. Fig. 3). Therefore, evidently, by changing the position of the current sensors, the analysis must be revised, but the same reasoning is maintained.

Fig. 13 shows a detail of the currents on the source side (i_{s+}, i_{sN}, i_{s-}), highlighting the average values and the ripple. Also in this case, the currents are balanced for the same average value on the positive (i_{s+}) and negative (i_{s-}) wires, while is zero in the neutral wire (i_{sN}). As shown, four different stages are identified (i to iv). The currents in the coupling filters L_a and L_b are presented in Fig. 14, while the detail of the ripple of such currents is presented in Fig. 15, in accordance with the switching of the IGBTs *b* and *c* (s_b and s_c). In this case, on the load side, as i_{l-} is half of i_{l+}, the current in L_a (i_{La}) is half of the current in L_b (i_{Lb}), since DC-DC #1 is linked to 800 V and DC-DC #2 to 400 V, operating, respectively in buck and boost mode. As shown, in both cases, when the IGBTs are turned *off*, the inductors store energy, while when the IGBTs are turned *on*, the energy is delivered to the circuit.

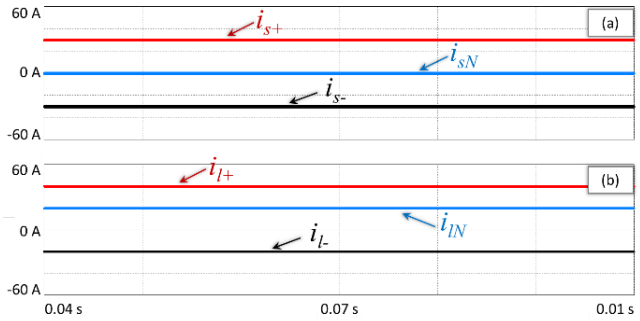


Fig. 12. Validation considering that the power in the top load is higher than the power in the bottom load: (a) Currents on the DCPG side (i_{s+}, i_{sN}, i_{s-}); (b) Currents on the load side (i_{l+}, i_{lN}, i_{l-}).

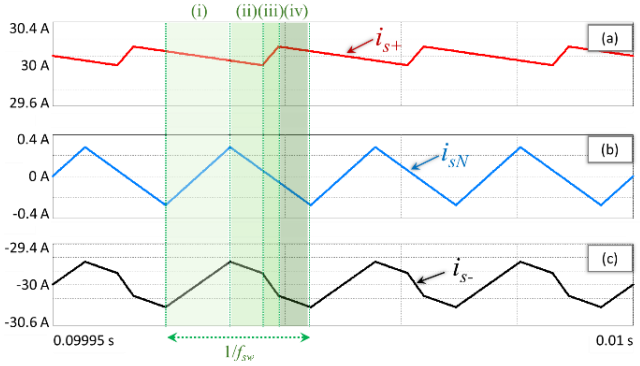


Fig. 13. Validation considering that the power in the top load is higher than the power in the bottom load, showing the detail of the average and ripple values: (a) Current i_{s+}; (b) Current i_{sN}; (c) Current i_{s-}.

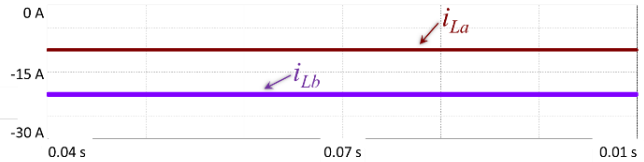


Fig. 14. Validation considering that the power in the top load is higher than the power in the bottom load, showing the currents in the coupling inductors, namely i_{La} and i_{Lb}.

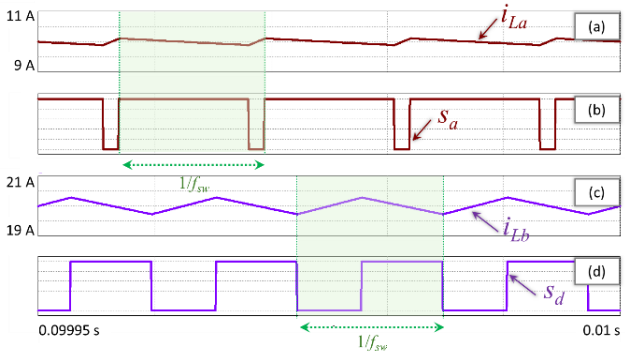


Fig. 15. Validation considering that the power in the top load is higher than the power in the bottom load, showing the detail of the ripple in the currents i_{La} and i_{Lb}, as well as the PWM of the IGBTs s_b and s_c.

V. Conclusion

DC power grids (DCPG) are becoming progressively noteworthy, principally due to the natural DC operation of technologies such as renewable energy, energy storage systems, and electric vehicles. Specifically, bipolar DCPGs are gaining prominence because they offer higher flexibility to accommodate DC technologies with distinct voltage levels and higher reliability. This is primarily due to the capabilities of power electronics, which allow the establishment of different voltage levels designed for various DC loads. Nevertheless, ensuring balanced power operation for all loads in a bipolar DCPG is challenging, leading to issues with current imbalances. This paper proposes an active current balancer (ABC) for ensuring balanced source currents in the bipolar DCPG, when the currents on the load side are unbalanced. The details of the digital control are presented for all possible scenarios, and the validation proves the correct operation of the DC-DC ABC operating with different current imbalances in the load side, namely with higher currents on the positive wire compared to the negative wire and vice-versa. For all cases, it was demonstrated that the current on the neutral wire is zero after the compensation performed by the DC-DC ABC. The validation is also performed both in steady-state and transient-state.

Acknowledgement

This work has been supported by FCT—Fundação para a Ciência e Tecnologia within the R&D Unit Project of ALGORITMI Centre. This paper was supported by the Alliance for the Energy Transition (56) co-financed by the Recovery and Resilience Plan (PRR) through the European Union. This work is also part of the project that has received funding from the European Union's Horizon Europe research and innovation program under the Marie Sklodowska-Curie Doctoral Networks grant agreement No 101072414 (E2GO). Sergio Coelho is supported by the doctoral scholarship 2021.08965.BD, granted by FCT—Fundação para a Ciência e Tecnologia.

References

[1] F. Aminifar et al., "Driving Innovation: Leveraging cloud platforms for grid modernization," in IEEE Electrification Magazine, vol. 13, no. 1, pp. 30-41, March 2025, doi: 10.1109/MELE.2025.3534458.

[2] M. Liserre, M. A. Perez, M. Langwasser, C. A. Rojas and Z. Zhou, "Unlocking the Hidden Capacity of the Electrical Grid Through Smart Transformer and Smart Transmission," in Proceedings of the IEEE, vol. 111, no. 4, pp. 421-437, April 2023, doi: 10.1109/JPROC.2022.3157162.

[3] K. M. Muttaqi, M. R. Islam and D. Sutanto, "Future Power Distribution Grids: Integration of Renewable Energy, Energy Storage, Electric Vehicles, Superconductor, and Magnetic Bus," in IEEE Transactions on Applied Superconductivity, vol. 29, no. 2, pp. 1-5, March 2019, Art no. 3800305, doi: 10.1109/TASC.2019.2895528.

[4] A. Mandal, K. M. Muttaqi, M. R. Islam and D. Sutanto, "Solid-State Power Substations for Future Power Grids," in IEEE Transactions on Industry Applications, vol. 61, no. 1, pp. 1055-1067, Jan.-Feb. 2025, doi: 10.1109/TIA.2024.3477447.

[5] R. Morello, C. De Capua, G. Fulco and S. C. Mukhopadhyay, "A Smart Power Meter to Monitor Energy Flow in Smart Grids: The Role of Advanced Sensing and IoT in the Electric Grid of the Future," in IEEE Sensors Journal, vol. 17, no. 23, pp. 7828-7837, 1 Dec.1, 2017, doi: 10.1109/JSEN.2017.2760014.

[6] M. Esmaeili, A. Anvari-Moghaddam, S. M. Muyeen and V. S. Perić, "On the Role of Renewable Energy Policies and Electric Vehicle Deployment Incentives for a Greener Sector Coupling," in IEEE Access, vol. 10, pp. 53873-53893, 2022, doi: 10.1109/ACCESS.2022.3176012.

[7] A. K. Karmaker, M. A. Hossain, H. R. Pota, A. Onen and J. Jung, "Energy Management System for Hybrid Renewable Energy-Based Electric Vehicle Charging Station," in IEEE Access, vol. 11, pp. 27793-27805, 2023, doi: 10.1109/ACCESS.2023.3259232.

[8] V. Monteiro, J. C. Ferreira, A. A. N. Meléndez, and J. L. Afonso, "Electric Vehicles On-Board Battery Charger for the Future Smart Grids," IFIP Advances in Information and Communication Technology, pp. 351–358, 2013, doi: 10.1007/978-3-642-37291-9_38.

[9] M. H. Saeed, W. Fangzong, B. A. Kalwar and S. Iqbal, "A Review on Microgrids' Challenges & Perspectives," in IEEE Access, vol. 9, pp. 166502-166517, 2021, doi: 10.1109/ACCESS.2021.3135083.

[10] H. Faraji, G. B. Gharehpetian, A. Khorsandi, S. Hossein Hosseinian, R. AhmadiAhangar and A. Rosin, "Active and Reactive Power Multi-Objective Control of Multi-Microgrid in On- and Off-Grid Modes," in IEEE Access, vol. 13, pp. 56531-56546, 2025, doi: 10.1109/ACCESS.2025.3553402.

[11] P. Wang, L. Goel, X. Liu and F. H. Choo, "Harmonizing AC and DC: A Hybrid AC/DC Future Grid Solution," in IEEE Power and Energy Magazine, vol. 11, no. 3, pp. 76-83, May-June 2013, doi: 10.1109/MPE.2013.2245587.

[12] M. Haddadi, S. A. Gorji and S. S. Yu, "An Overview of Inertia Emulation Strategies for DC Microgrids: Stability Analysis and AC Microgrid Analogies," in IEEE Open Journal of the Industrial Electronics Society, vol. 6, pp. 491-521, 2025, doi: 10.1109/OJIES.2025.3550625.

[13] D. Van Hertem et al., "Substations for Future HVdc Grids: Equipment and Configurations for Connection of HVdc Network Elements," in IEEE Power and Energy Magazine, vol. 17, no. 4, pp. 56-66, July-Aug. 2019, doi: 10.1109/MPE.2019.2909006.

[14] Moslem Uddin, Huadong Mo, Daoyi Dong, Sondoss Elsawah, Jianguo Zhu, Josep M. Guerrero, "Microgrids: A review, outstanding issues and future trends," Elsevier Energy Strategy Reviews, vol.49, pp.101-127, Sept. 2023, doi: 10.1016/j.esr.2023.101127.

[15] V. F. Pires, D. Foito, A. Cordeiro and A. J. Pires, "A Bidirectional DC-DC Converter to Interlink Unipolar and Bipolar DC Microgrids," 9th International Conference on Smart Grid, Setubal, Portugal, 2021, pp. 37-42, doi: 10.1109/icSmartGrid52357.2021.9551209.

[16] Cátia F. Oliveira, João L. Afonso, Vítor Monteiro, "A Bidirectional Multilevel DC-DC Converter Applied to a Bipolar DC Grid: Analysis of Operation under Fault Conditions", IEEE YEF-ECE 2021 - International Young Engineers Forum, Almada, Portugal, July 2021, pp.39-43, doi: 10.1109/YEF-ECE52297.2021.9505140.

[17] O. Husev, D. Vinnikov, S. Kouro, F. Blaabjerg and C. Roncero-Clemente, "Dual-Purpose Converters for DC or AC Grid as Energy Transition Solution: Perspectives and Challenges," in IEEE Industrial Electronics Magazine, vol. 18, no. 1, pp. 46-57, March 2024, doi: 10.1109/MIE.2022.3230219.

[18] Vítor Monteiro, Cátia F. Oliveira, João L. Afonso, "A Multilevel Bidirectional Four-Port DC-DC Converter to Create a DC-Grid in Solid-State Transformers with Hybrid AC/DC Grids", IEEE YEF-ECE 2021 - International Young Engineers Forum, Almada, Portugal, July 2021, pp.26-31, doi: 10.1109/YEF-ECE52297.2021.9505158.

[19] H. Jia, Q. Xiao and J. He, "An Improved Grid Current and DC Capacitor Voltage Balancing Method for Three-Terminal Hybrid AC/DC Microgrid," in IEEE Transactions on Smart Grid, vol. 10, no. 6, pp. 5876-5888, Nov. 2019, doi: 10.1109/TSG.2018.2834340.